PHYSIOLOGICAL ECOLOGY - ORIGINAL PAPER

Predicting lichen hydration using biophysical models

Anna V. Jonsson · Jon Moen · Kristin Palmqvist

Abstract Two models for predicting the hydration status of lichens were developed as a first step towards a mechanistic lichen productivity model. A biophysical model included the water potential of the air, derived from measurements of air temperature, relative humidity and species-specific rate constants for desiccation and rehydration. A reduced physical model, included only environmental parameters, assuming instantaneous equilibration between the lichen and the air. These models were developed using field and laboratory data for three green algal lichens: the foliose epiphytic *Platismatia glauca* (L.) W. Culb., the fruticose epiphytic *Alectoria sarmentosa* (Ach.) Ach. and the fruticose, terricolous and mat-forming *Cladina rangiferina* (L.) Weber ex Wigg. The models were compared and validated for the same three species using data from a habitat with a different microclimate. Both models predicted the length and timing of lichen hydration periods, with those for *A. sarmentosa* and *P. glauca* being highly accurate—nearly 100% of the total wet time was predicted by both the biophysical and physical models. These models also predicted an accurate timing of the total realized wet time for *A. sarmentosa* and *P. glauca* when the lichens were wet. The model accuracy was lower for *C. rangiferina* compared to the epiphytes, both for the total realized wet time and for the accuracy of the timing for the hydration period. These results demonstrate that the stochastic and continually varying hydration status of lichens can be simulated from biophysical data. Further

development of these models to also include water-related activity, light and temperature conditions during the hydration events will then be a potent tool to assess potential lichen productivity in landscapes and habitats of various microclimatic conditions.

Introduction

Lichens are increasingly threatened by environmental changes ranging from climate change (Epstein et al. 2004) to increased nitrogen deposition (Söchting 1995) and forestry practices (Esseen et al. 1996, Saunders et al. 1991). To predict lichen responses to these changes, we need models that can simulate lichen performance under various environmental conditions. Since lichens are poikilohydric, their growth is primarily limited by the length and frequency of their wet active periods together with the irradiance received during these events (Palmqvist and Sundberg 2000; Dahlman and Palmqvist 2003). Any growth model for these organisms must therefore be able to incorporate their varying hydration status over time (Coxson 1991). Lichen water relations have been extensively studied both in the field and in the laboratory (Heatwole 1966; Kershaw and Rouse 1971a; Blum 1973; Larson 1981; Rundel 1982; Lange et al. 1986, 1993, 2006; Green et al. 1991, 1994; Schroeter and Scheidegger 1995; Gauslaa and Solhaug 1998; Zotz et al. 1998; Fos et al. 1999; Lalley and Viles 2006). Despite an abundance of data, however, we still lack an easily applicable and mechanistic model that simulates the loss and uptake of water for longer time periods in situ based on variables that can be easily

A. V. Jonsson (✉) · J. Moen · K. Palmqvist
Department of Ecology and Environmental Science,
Umeå University, 901 87 Umeå, Sweden
e-mail: anna.jonsson@emg.umu.se

obtained and quantified (see Rundel 1982). Recent models of lichen productivity have been merely empirical, assessing metabolic active time from direct measurements of thallus water content using an impedance technique (Coxson 1991; Palmqvist and Sundberg 2000; Sundberg et al. 2001; Dahlman and Palmqvist 2003; Gaio-Oliveira et al. 2003, 2006). Although this is a robust method, it is technically complex and merely descriptive, giving an after-the-fact relationship between climate and growth that cannot be used for predictions.

The hydration of lichen thalli can be achieved from rain, high air humidity, fog or dew (Rundel 1988), i.e. water sources that can differ significantly between habitats and seasons. Further, lichen water loss and uptake are physical processes without metabolic control (Blum 1973) with the thallus water content passively equilibrating with the free energy of water in the surrounding air (see Rundel 1982). We therefore hypothesized that lichen water content is primarily controlled by the water potential of the air (ψ_{air}), which is determined by the air relative humidity (RH) and temperature (T_{air}). However, lichen water relations are also passively influenced by species-specific morphological and anatomical characters (Larson and Kershaw 1976; Larson 1981; Valladares et al. 1993; Valladares 1994; Maguás et al. 1997; Gauslaa and Solhaug 1998), and this must also be considered when modeling lichen growth. Further, growth site and/or growth structure (e.g. mat-forming lichens) can alter the atmospheric conditions by increasing the boundary layer, thereby prolonging the hydration periods (Kershaw and

Field 1975; Larson and Kershaw 1976; Gates 1980; Zotz et al. 2000).

The aim of this study was to develop a mathematical and mechanistic model predicting the length and occurrence of wet active periods in situ in lichens with green algal photobionts. This hydration model would then provide a first step towards a generalized and mechanistic lichen productivity model. We developed models using a combination of meteorological data, in situ thallus water content measurements and laboratory measurements of species-specific characteristics for the foliose epiphytic *Platismatia glauca* (L.) W. Culb., the fruticose epiphytic *Alectoria sarmentosa* (Ach.) Ach. and the fruticose, terricolous and mat-forming *Cladina rangiferina* (L.) Weber ex Wigg. We specifically asked whether their water dynamics could be predicted from simple environmental parameters or in combination with species-specific characteristics. We hypothesized that this simple approach would fit better for the epiphytic lichens with a high coupling to the atmospheric conditions compared to the mat-forming lichen.

Material and methods

Lichen material

Three lichens with green algal *Trebouxia* photobionts were chosen for the modeling (Fig. 1c–e). The foliose epiphytic *Platismatia glauca* (L.) W. Culb. has a wide habitat

Fig. 1 Overview of the two field sites Kulbäcksliden (**a**) and Åheden (**b**), thallus size and appearance of *Alectoria sarmentosa* (**c**), *Platismatia glauca* (**d**) and *Cladina rangiferina* (**e**), when equipped with the water content (WC)-measuring clips and a light sensor. The light sensors were used for purposes outside this study
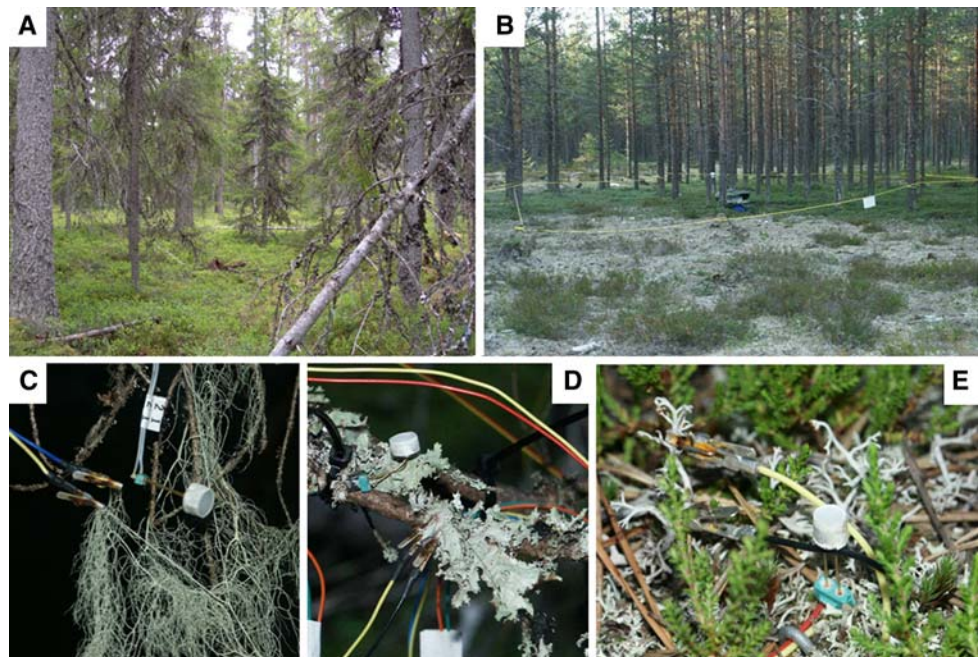
tolerance and is common on Norway spruce (*Picea abies*) in boreal forests. The thallus is thin and loosely attached to the substrate so exposure to the surrounding air is relatively high. The fruticose, pendulous, epiphytic *Alectoria sarmentosa* (Ach.) Ach. is less common in Scandinavia compared to *P. glauca* and is often confined to old growth forests with long continuity (Esseen et al. 1996). The thallus is dichotomously branched and hangs loosely over twigs and needles, generally on Norway spruce. Exposure to the air is higher for *A. sarmentosa* than for *P. glauca* because of its pendulous growth form and potentially higher surface-to-area ratio. The fruticose, terricolous and mat-forming lichen *Cladina rangiferina* (L.) Weber ex Wigg. is a wide-spread species on nutrient-poor, exposed pine heaths. A *Cladina*-mat can be up to 10–12 cm deep with only the uppermost parts being directly exposed to the surrounding air; the lower parts of older thalli are often more or less decayed. It has been suggested that the density and thickness of the lichen-mat function as water reservoirs and reduce desiccation rates (Kershaw and Rouse 1971a, b; Kershaw and Field 1975), although Gaio-Oliveira et al. (2006) found no such effect.

Study sites

The three study sites (Table 1), one dense spruce-dominated forest (Omagaliden), one pine heath (Åheden, Fig. 1b) and one old-growth and open mixed forest stand (Kulbäcksliden, Fig. 1a), all situated 50–60 km to the north-west of Umeå, represented an as wide as possible climatic gradient for the lichens within easy reach for continuous visits and maintenance. Because of different habitat preferences, *C. rangiferina* was absent from Omagaliden, while *A. sarmentosa* and *P. glauca* were absent from Åheden (Table 1). Omagaliden was a dense 70- to 80-year-old forest located on a north-facing slope above Vindelälven; it was dominated by spruce and pine, intermixed with *Salix caprea*, *Sorbus aucuparia*, *Populus tremula* and *Betula* spp., with a lush epiphytic lichen flora. Kulbäcksliden was an open old-growth stand with a tree composition similar to that of Omagaliden and a dwarf-shrub ground vegetation dominated by bilberry (*Vaccinium myrtillus*) and bryophytes with intermixed patches of the *Cladina* community. The epiphytic flora was similar to that of Omagaliden, with large thalli of pendulous lichens being dominant in older spruce trees. Åheden was dominated by even-aged, even-sized pines with a stem diameter at breast-height of less than 10 cm; it harbored a sparse *Cladina*-lichen community of approximately 5 cm in height in an early successional stage (Kumpula 2001) due to reindeer grazing. At sheltered sites below the tree canopy, the lichen mat was intermixed with lingonberries (*Vaccinium vitis-idaea*) and scattered patches of the moss *Hylocomium splendens*.

Field measurements

Water relations of the three lichens were measured with an impedance technique on native thalli without removing them from their natural substrate (Coxson 1991; Renhorn et al. 1997) in which two silver-plated crocodile clips with a contact area of 3 × 2 mm were placed a few millimeters apart on the lichen thallus (Fig. 1). The experiment was designed to measure the water content (WC) of both exposed and shaded thalli of the two epiphytes at each site (Table 1) using thalli positioned 0.7–2.2 m above the ground. For *C. rangiferina*, measurements were made both on the more exposed parts of the mat and on smaller cushions embedded in bryophytes. The 2.5-V alternating current applied every minute can cause some necrosis, so the clips where moved to a fresh thallus at the first sign of necrosis during the experiment.

A data logger (CR 10, Campbell Scientific, Logan UT), supplemented with a Relay Multiplexer (AM 416; Campbell Scientific), was placed at each of the three above sites between 16 June and 1 October, 2004. In addition to measuring thallus WC, this data logger also recorded air temperature and relative air humidity with a probe (Hygroclip S3; Rotronic AG, Bassersdorf, Switzerland) that was equipped with a radiation shield and a ventilating fan and placed at the center of each experimental site 0.5 ± 0.1 m above the ground. Irradiance in the spectral range of 190–680 nm was recorded with Gallium-arsenide-phosphide photodiodes (effective area 5.6 mm^2; G1126–02; Hammamatsu Photonics, Hammamatsu City, Japan) that were covered by a white diffuser disc to obtain a cosine response (Ø = 8 mm). Precipitation was measured with a rain-gauge (ARG100; Environmental Measurements, Wearfield, Sunderland, UK) placed in an open canopy gap within 10 m of the lichens at Omagaliden. Precipitation at Kulbäcksliden and Åheden was obtained from other climate stations (Svartberget experimental forests, Vindeln, Sweden), placed 500 and 100 m from the respective experimental site. The physical parameters were measured at 1-min intervals and stored as 15-min averages, except for rain, which was summed. All sites were visited at least once weekly to collect the data, check for broken sensors and to adjust the WC-clips if necessary.

The WC data were processed on a relative scale between maximal and minimal conductivity for each thallus-clip set-up; fully hydrated thalli were defined as 100% WC and dry thalli as 0%. Water content values in-between these two extremes were derived using a linear equation for each lichen-clip set-up, as detailed by previous researchers (e.g. Palmqvist and Sundberg 2000; Gaio-Oliveira et al. 2006). Because heavy rainstorms may create a transient water film on the thallus surface and short-circuit the conductivity measurements, the data were "de-spiked" before the

Table 1 Geographical position and climatic conditions during the experimental period (June 16 to October 1, 2004) at the three field sites

Parameter	Omagaliden	Kulbäcksliden	Åheden	
Geographical position	64°09′N, 19°50′E	64°10′N, 19°30′E	64°11′N, 19°40′E	
Site characteristics Climatic variables	Dense mixed spruce	Open mixed spruce	Exposed pine-heath	
I_{tot} (mol photons m^{-2})[a]	58 ± 9 [12]	219 ± 42 [12]	647 ± 75 [12]	
Minimum ψ_{air} (MPa)	−123	−149	−176	
Mean ψ_{air} (MPa)	−16	−25	−29	
Maximum T_{air} (°C)	24.5	27.3	27.3	
Mean T_{air} (°C)	11.6	11.4	11.1	
Min T_{air} (°C)	−0.3	−1.5	−4.2	
Precipitation (mm)	344	381	332	
Species			Embedded	Exposed
Alectoria sarmentosa				
Measured thalli	6 (3E, 3S)[b]	4 (2E, 2S)[b]	–	–
Wet time (h)	1548 ± 138	923 ± 84		
I_{wet} (mol m^{-2})	20.9 ± 3.3	32,3 ± 10.2		
Mean T_{wet} (°C)	10.2	9.7		
	P[c]	V[c]		
Platismatia glauca				
Measured thalli	6 (3E, 3S)[b]	5 (2E, 2S)[b]	–	–
Wet time (h)	1150 ± 31	975 ± 24		
I_{wet} (mol m^{-2})	35.1 ± 7.4	39.8 ± 10.6		
Mean T_{wet} (°C)	10.4	9.7		
	P[c]	V[c]		
Cladina rangiferina				
Measured thalli	–	5 (2E, 2S)[b]	6	6
Wet time (h)		1740 ± 74	1674 ± 88	1289 ± 27
I_{wet} (mol m^{-2})		196 ± 46	302 ± 35	362 ± 51
Mean T_{wet} (°C)		10.1	9.4	10.1
		P[c]	V[c]	V[c]

Additional site characteristics and measurements and processing of the climatic variables are presented in the Material and methods. Micro-climatic conditions (mean ± SE) for each lichen species and field site are given for the number of thalli used for measurements and the site used for parameterization or validation

[a] The total irradiance, I_{tot}, close to the lichen thallus represents the mean ± 1 SE for the number [n] of sensors mounted close to the experimental thalli at each site (see Fig. 1)

[b] E number of exposed thalli at each site; S, number of shaded at each site

[c] P that data was used for parameterization of the model; V, that data used for validation of the model

maximal hydration values were extracted. The water potential of the air was calculated using Eq. 1, modified from Nobel (1999) by neglecting the adjustment for altitude,

$$\psi_{air} = \frac{RT_{air}}{V} \ln\left(\frac{RH}{100}\right) \quad (1)$$

where ψ_{air} is the air water potential (Pa), R is the gas constant (8.31441 J mol K^{-1}), T_{air} is the air temperature (K), V is the partial molar volume of water (18.021 × 10^{-6} m^{3}mol^{-1} at 10°C) and RH is the relative humidity of the air (percentage) (see also abbreviations and definitions used in Table 2).

Laboratory measurements

The species-specific desiccation and rehydration kinetics were determined under laboratory conditions using lichens from the field sites that had been brought to the laboratory, rinsed of debris, dried in darkness at 15°C and 40% RH for 24 h and stored in a freezer (−18°C) for a few weeks

Table 2 Mathematical terms, abbreviations and definitions used in this paper

Name	Symbol	Value	Units
Air temperature	T_{air}		°C
Relative humidity of the air	RH		%
Water potential of the air	ψ_{air}		MPa
Ambient water content of the thallus	WC_{amb}		%
Water content of water saturated thallus	WC_{sat}	100	%
Water content of thallus in equilibrium with ψ_{air}	WC_{eq}		%
Water content of desiccated thallus	WC_0	0	%
Water binding constant	w_{eq}		MPa^{-1}
Rate constant for desiccation	k_{des}		min^{-1}
Rate constant for rehydration in humid air	k_{reh}		min^{-1}
Thallus fresh weight at WC_{sat}	FW_{sat}		g
Dry weight of desiccated thallus	DW_{des}		g
WC range for hydrated thallus	WC_{wet}	5–100	%
Irradiance intercepted by hydrated thalli	I_{wet}		mol photons m^{-2}
Total irradiance over experimental period	I_{tot}		mol photons m^{-2}

Values are given when appropriate, or otherwise presented in the text or tables

before the measurements were taken. The frozen thalli were then equilibrated in their dry state at room temperature for 24 h and dried in a desiccator over silica gel to determine their dry weight (DW_{des}). Sample DW varied between 0.18 and 0.42 g for *A. sarmentosa*, between 0.04 and 0.26 g for *P. glauca* and between 0.44 and 2 g for *C. rangiferina*. Full hydration was obtained by spraying the lichen with water and then placing it on a soaked dishcloth for 3 h at 20°C. Excess water was removed by a quick shaking of the thallus prior to the weighing. Thallus WC during the laboratory measurements was obtained gravimetrically, using Eq. 2 to derive the relative WC, thus allowing direct comparisons with the field conductivity data.

$$WC = \frac{(FW - DW_{des})}{(FW_{sat} - DW_{des})} \times 100 \quad (2)$$

where WC is the current relative water content, FW is the current fresh weight, DW_{des} was derived as described above, and FW_{sat} is the fresh weight of the thallus when fully hydrated (Table 2). Calibration of the conductivity method in relation to the gravimetrical method was made by combining the two techniques in the laboratory during a desiccation event (see inserted figures for each species in Fig. 2). When wet, the crocodile clips retain moisture longer than the rest of the thallus and therefore record stronger signals than expected; in contrast, when almost dry, the water is unevenly distributed in the thallus, being retained longer in the interior parts than at the margins. Hence, since the clips are attached to the thallus margin, the conductivity method will underestimate the lower thallus WCs and overestimate the higher WCs. Consequently, since the sigmoidal relationship between the two techniques is simply a technical artifact, we applied a more realistic linear relationship instead (Fig. 2), one in which the relationship would likely have a better fit than that due to this clip-effect. Desiccation kinetics were obtained by placing fully hydrated thalli in a climate room at a ψ_{air} of −92.5 MPa (7.7°C, 49% RH; measured using the field equipment) and exposing the thalli directly to the surrounding air, with repeated weighings for 8 h.

Rehydration kinetics were obtained using desiccated thalli placed in 2-l, 13-cm-wide and 23-cm-high sealed glass cylinders containing 250 ml of water, which was continuously stirred with a magnetic stirrer, placed in the climate room, creating a ψ_{air} of −4 MPa (97% RH and 10°C; measured immediately after each experiment).

The models

The models were based on the following assumptions: (1) since lichens absorb and lose water passively (Blum 1973), their WC is closely coupled to prevailing atmospheric water conditions; (2) the water potential of the lichen equilibrates asymptotically with the water potential of the air (ψ_{air}), thus accounting for both the humidity and temperature of the air (Eq. 1), where water moves along a decreasing water potential gradient between the lichen and the air (Rundel 1982); (3) lichen WC was assumed to be a direct function of the lichen water potential, which enables modeling for lichen WC instead of the more difficult to measure lichen water potential; (4) based on the definition of passive diffusion, the rates of lichen water loss and uptake are directly proportional to the difference between the ambient water content (WC_{amb}) of the lichen thallus and the equilibrium water content (WC_{eq}); (5) the rate constants of water uptake and loss may be species-specific
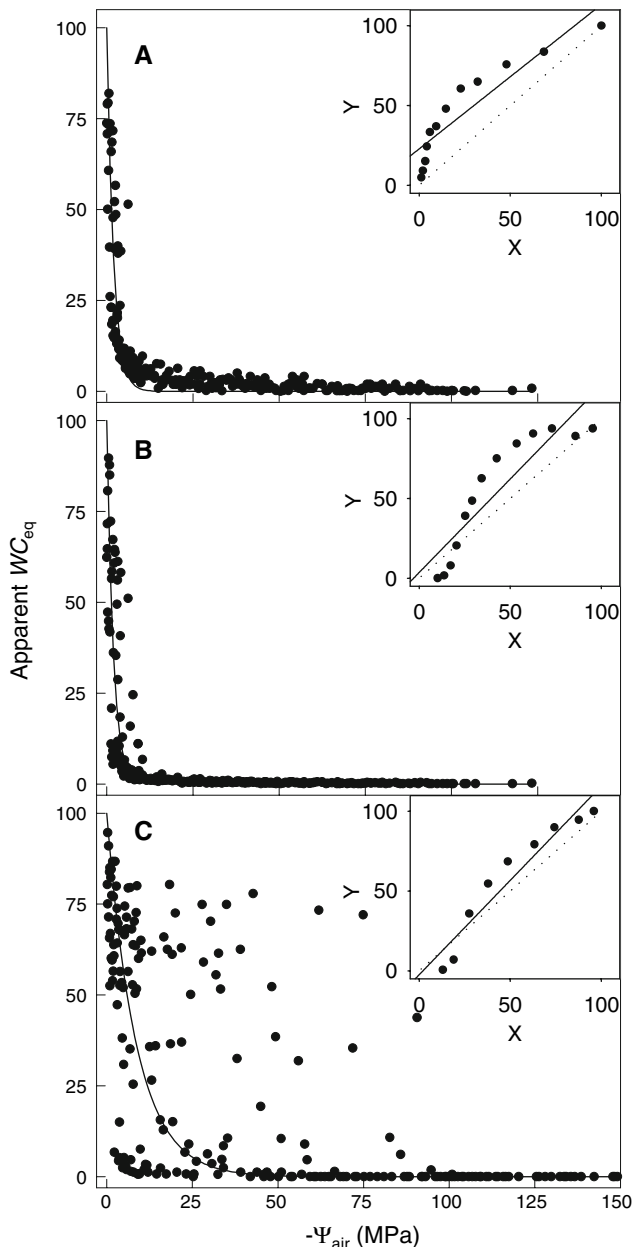
Fig. 2 Relationships between the negative water potential of the air ($-\psi_{air}$) and the apparent equilibrium water content (WC_{eq}) for *A. sarmentosa* (**a**), *P. glauca* (**b**) and *C. rangiferina* (**c**), extracted from the field data as described in the Material and methods. An exponential decay function of the form $WC_{eq} = WC_{sat}e^{w_{eq}\cdot\psi_{air}}$ (Eq. 3) was fitted to the data, where the parameter w_{eq} is a species-specific constant specifying the shape of the curve (Table 3). WC_{sat} was set to 100%. *Inserted* figures show examples of the relationship between relative WC measured by weight (%) (*X*-axis) and conductivity (%) (*Y*-axis) for each species. The *dotted line* represents the theoretical 1:1 fit between *X* and *Y*. Adjusted r^2 values for the linear regressions are 0.83 (*A. sarmentosa*), 0.79 (*P. glauca*) and 0.91 (*C. rangiferina*)

since they are related to thallus resistance (Gates 1980); (6) the desiccation and rehydration rates have to be modeled separately since they may differ (Mutch and Gastineau 1970) .

Since the lichen WC was assumed to be a direct function of the lichen water potential, the WC_{eq} was also assumed to be a direct function of ψ_{air}. The relationship between WC_{eq} and ψ_{air} was empirically determined using field data (Fig. 2), as described later in this section, yielding the following general function (Eq. 3):

$$WC_{eq} = WC_{sat}e^{w_{eq}\cdot\psi_{air}} \tag{3}$$

where WC_{eq} (%) is the water content of the thallus in equilibrium with the air, WC_{sat} (%) is the water content of the water-saturated thallus (100%), ψ_{air} is the water potential of the air (MPa)and w_{eq} (MPa^{-1}) is a species-specific water-binding constant (Table 3).

The rate of water movement between the lichen and the air during desiccation and rehydration can be expressed as Eq. 4:

$$\frac{\partial WC}{\partial t} = -k\left(WC_{amb} - WC_{eq}\right) \tag{4}$$

where WC_{amb} (%) is the ambient water content and WC_{eq} (%) is the water content at equilibrium derived from Eq. 3, and k (min^{-1}) is the rate constant for desiccation (k_{des}) or rehydration (k_{reh}), (Fig. 3, Table 3).

Inserting Eq. 3 into Eq. 4 yields Eq. 5:

$$\frac{\partial WC}{\partial t} = -k\left(WC_{amb} - WC_{sat}e^{w_{eq}\cdot\psi_{air}}\right) \tag{5}$$

Two models were built using the above assumptions and equations. The first model, hereafter referred to as the biophysical model, was built on all of the above assumptions and Eqs. 3–5. The second model, denoted the physical model, was reduced by assuming instantaneous equilibrium—hence no time delay between ambient WC and WC_{eq}. This was implemented by replacing WC_{eq} with WC_{amb} in Eq. 3. Both models were developed for each of the three species.

Model parameterization, analyses and simulations

Parameterization of Eq. 3 was made using field-data from June to October obtained from the most sheltered experimental site for each species (Table 1). The thalli were randomly chosen and included both exposed and shaded or embedded specimens (Table 1). Because ψ_{air} was constantly changing during the field conditions, sufficient time for WC equilibration at a fixed ψ_{air} was seldom realized. The following procedure was adopted to sample values as close to equilibrium as possible—i.e. the apparent equilibria. Consider a desiccation sequence where ψ_{air} drops and the lichen WC follows with a time-lag; the closest value to a true WC_{eq} will then occur when the ψ_{air} starts to increase again. Based on examination of the data sets, this turning point was used as a sampling point when the WC
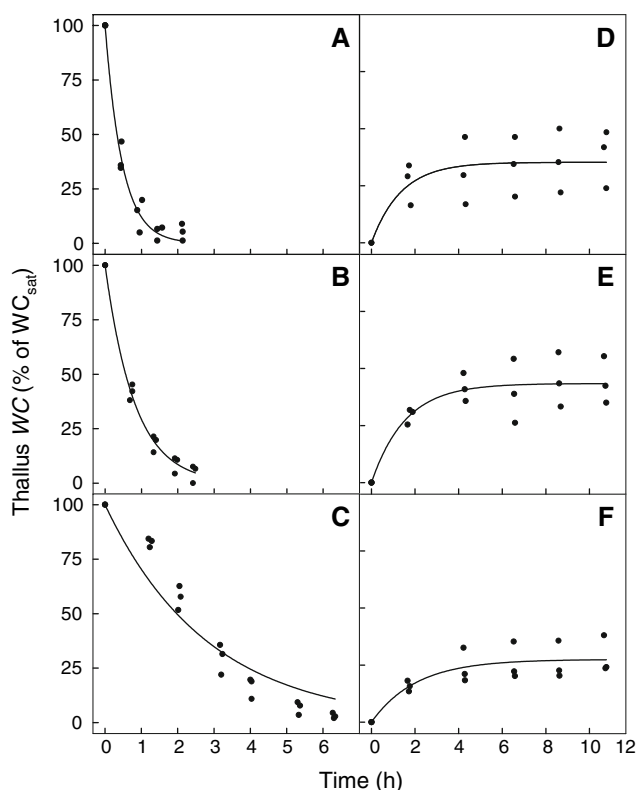
Fig. 3 Desiccation kinetics (**a–c**) of fully hydrated thalli at a ψ_{air} of −92.5 MPa (T_{air} 7.8°C, RH 49%) and rehydration kinetics (**d–f**) of dry thalli at a ψ_{air} of −4.0 MPa (T_{air} 10°C, RH 97%) for *A. sarmentosa* (**a, d**), *P. glauca* (**b, e**) and *C. rangiferina* (**c, f**). An exponential decay function of the form $WC = WC_{sat} \cdot e^{-k_{des} \cdot t}$ (Eq. 6) was fitted to the desiccation time-series, where the parameter k_{des} is a species-specific constant specifying the shape of the curve. WC_{sat} was set to 100%. A non-linear function of the form $WC = WC_{eq}(1 - e^{k_{reh} \cdot t})$ (Eq. 7) was fitted to the rehydration time-series where k_{reh} is a species-specific constant specifying the shape of the curve. WC_{eq} is the equilibrium WC at the particular ψ_{air}. Parameter values for each species are presented in Table 3

was lower than all points 60 min before (*A. sarmentosa* and *P. glauca*) or lower than all points 120 min before (*C. rangiferina*). The reverse procedure was used for the

rehydration sequences. The apparent $WC_{eq}-\psi_{air}$ data-pairs were thereafter divided into step-wise ψ_{air} intervals: each interval being 0.2 MPa wide in the 0 to −10 MPa range and 1 MPa wide when ψ_{air} was below −10 MPa. For the desiccation periods, the lowest apparent WC_{eq} value in each interval was defined as the apparent equilibrium value, while the highest apparent WC_{eq} value was used for the rehydration periods. To yield the $WC_{eq}-\psi_{air}$ relationship for Eq. 3, the two reduced data sets—i.e. for both rehydration and desiccation—were then pooled, and an exponential decay function was fitted to the values (Fig. 2). The data was extracted using MATLAB (R2006a; The MathWorks, Natick, USA).

Parameterization of the rate constant k (k_{des} and k_{reh}) was made using the laboratory data presented in Fig. 3 and Table 3. The k_{des} values were derived by least-squares regression fits (SIGMAPLOT ver. 8.0; Systat Software, Richmond, CA) to the desiccation time-series (Fig. 3) using Eq. 6:

$$WC = WC_{sat} \cdot e^{-k_{des} \cdot t} \tag{6}$$

where t is time (min). The k_{reh} values were derived by least-squares regression fits of Eq. 7 to the rehydration time-series (Fig. 3):

$$WC = WC_{eq}\left(1 - e^{k_{reh} \cdot t}\right) \tag{7}$$

The fits to Eqs. 6 and 7 are in accordance with Eq. 4 and supported by data presented by Mutch and Gastineau (1970).

To analyze the model, the relative sensitivity of WC to the parameters k, w_{eq} and ψ_{air} (Eqs. 8–10) was evaluated by an elasticity analysis of Eq. 5 for the desiccation and rehydration processes, respectively. The elasticity (e) of WC to a change in a parameter (a) is defined as the partial derivative of WC with respect to a, rescaled to account for the magnitude of both WC and a. Thus, e predicts the proportional change in WC given a proportional, infinitesimal change in a. We evaluated the absolute value of e

Table 3 Parameters of the non-linear equations obtained from the data presented in Figs. 2, 3, where w_{eq} is a species-specific water-binding constant for the $\psi_{air}-WC_{eq}$ relation (see Eq. 3), k_{des} is the rate constant for desiccation at a water potential resulting in a thallus WC close to 0 and k_{reh} is the rate constant for rehydration at a water potential resulting in the uptake of water by a dry thallus

Parameter	*A. sarmentosa*	*P. glauca*	*C. rangiferina*
w_{eq} (MPa^{-1})	0.51 ± 0.028	0.53 ± 0.037	0.12 ± 0.016
Adjusted r^2	0.74	0.64	0.30
k_{des} (min^{-1})	0.036 ± 0.002	0.021 ± 0.001	0.0059 ± 0.0006
Adjusted r^2	0.98	0.99	0.92
k_{reh} (min^{-1})	0.0082 ± 0.0044	0.0072 ± 0.0023	0.0054 ± 0.0020
WC_{eq} (%) at −4 MPa	35.3 ± 3.4	43.4 ± 2.8	27.5 ± 2.3
Adjusted r^2	0.60	0.80	0.75

Values represent the mean ± 1 SE of three individual thalli of each species

since we were interested in the magnitude of the elasticity regardless of the direction of the perturbation:

$$e_k = \left| \frac{k}{\text{WC}} \frac{\partial \text{WC}}{\partial k} \right| \tag{8}$$

$$e_\psi = \left| \frac{\psi}{\text{WC}} \frac{\partial \text{WC}}{\partial \psi} \right| \tag{9}$$

$$e_{w_{\text{eq}}} = \left| \frac{w_{\text{eq}}}{\text{WC}} \frac{\partial \text{WC}}{\partial w_{\text{eq}}} \right| \tag{10}$$

The models were validated using field-data (ψ_{air}) from a more exposed site than where the data for the parameterizations were obtained (Fig. 2, Table 1). The recorded 15-min averaged data for ψ_{air} were then interpolated to obtain a continuous function for ψ_{air}. In the physical model, the thallus WC dynamics over time was thereby simulated for each species using ψ_{air} as the independent variable and the species-specific w_{eq} (Fig. 2, Table 3) to derive WC_{eq} (Eq. 3). For the biophysical model, the species-specific properties of desiccation and rehydration were added (Table 3), and the WC dynamics were simulated by integrating Eq. 5, by the ODE solver ode45 in MATLAB R2006a, continuously alternating between the rehydration and desiccation processes. Initial WC in the simulations was set to measure initial WC in the field. The simulated WC was subsequently compared with the WC derived from the conductivity measurements.

Results

Species parameters and elasticity

The w_{eq} constant was 0.51 MPa^{-1} for the two epiphytic lichens while it was lower, 0.12 MPa^{-1}, for the mat-forming *C. rangiferina* (Fig. 2, Table 3). The lower value was probably due to data scatter caused by the uncoupling between lichen mats and atmospheric conditions. The rate constant for desiccation, k_{des}, (Fig. 3a–c) differed significantly between all three species, with *A. sarmentosa* having the fastest rate (0.036 min^{-1}) and *C. rangiferina* the slowest (0.059 min^{-1}). The rate constant for rehydration (k_{reh}) (Fig. 3d–f) was more similar for the three lichens, and slower than the desiccation rate in the two epiphytic lichens (Table 3).

The relative sensitivity of lichen WC to each of the parameters ψ_{air}, w_{eq} and k varied during the course of a desiccation or rehydration (Fig. 4) event using the biophysical model. Both processes initially showed the most sensitivity to k, but thereafter they were equally sensitive to ψ_{air} and w_{eq}. The WC at the transition from k to ψ_{air} sensitivity was close to WC_{eq} in all simulations presented in Fig. 4 (not shown). The period required to reach WC_{eq}, during both

desiccation and rehydration, was increased when k was decreased, thereby slowing the processes down. In contrast, the two processes responded differently to an altered w_{eq} where equilibrium was reached faster during desiccation and slower during rehydration the lower the w_{eq} (Fig. 4).

Model validation

Both models simulated the measured WC values very well, catching both stochastic rain events as well as morning fog, dew or high humidity (hereafter denoted as humid air) in all three species (compare the wet periods induced by rain—day numbers 179 and 181—and the wet periods induced by sufficiently low ψ_{air}—day numbers 177 and 178) (Fig. 5). The agreement between simulated and measured values was better for the two epiphytic lichens than for the mat-forming *C. rangiferina*. Even though the dynamic changes in thallus WC was simulated rather accurately, the agreement between measured and simulated WC for the absolute WC level was less precise, with the biophysical model being more accurate during the humid air-events while the physical model more accurately followed water uptake induced by rain; this trend was especially evident in *C. rangiferina* (Fig. 5). The embedded thalli of *C. rangiferina* remained wet for longer periods than the exposed thalli and longer than was simulated by either of the two models (Fig. 5).

Lengths of hydrated periods

The ability of the models to predict hydration periods from the two different water sources, rain or humid air, was determined by comparing observed and simulated hydration periods induced by these sources. Since hydration periods induced by humid air never exceeded 20 h, while rain resulted in longer periods (not shown), the data were separated into these two time-frames (Fig. 6). The agreement between observed and simulated hydration period lengths was high when these were induced by rain; i.e. exceeded 20 h (Fig. 6a–d). The accuracy was particularly high for *A. sarmentosa*, with close to a 1:1 fit between the observed and simulated data (Table 4). In general, the models underestimated the observed hydration periods for the other two lichens, while still being relatively accurate for *P. glauca* and the exposed samples of *C. rangiferina*. Both models significantly underestimated the longest hydration periods resulting from rain for the embedded *C. rangiferina* (Fig. 6d, Table 4).

The accuracy between simulated and observed hydration periods was generally lower for the humid air events; i.e. periods shorter than 20 h (Fig. 6e–h), although they were

Fig. 4 Elasticity of WC to the parameters w_{eq} (*triangles*), ψ_{air} (*solid line*) and k (*dotted line*) during rehydration (**a**) of a dry lichen thallus at a ψ_{air} of -1 MPa and during desiccation (**b**) of a water-saturated lichen thallus at a ψ_{air} of -20 MPa. The elasticity of WC was simulated by elasticity analysis in which one parameter was varied at a time for 16.7 h (1000 min), see Material and methods. k was fixed (k_{reh}: 0.069 min^{-1}, k_{des}: 0.0206 min^{-1}) in the *upper* panels, with w_{eq} varying [0.6 (high), 0.35 (medium), 0.1 (low) MPa^{-1}], while w_{eq} was fixed (0.35 MPa^{-1}) in the *lower* panels, with k varying [k_{reh}: 0.011 (high), 0.0069 (medium), 0.0030 (low) min^{-1}, k_{des}: 0.04 (high), 0.0206 (medium), 0.006 (low) min^{-1}]. The constants were varied within the observed range for the three species (Table 3). See Table 2 for definitions of abbreviations and constants
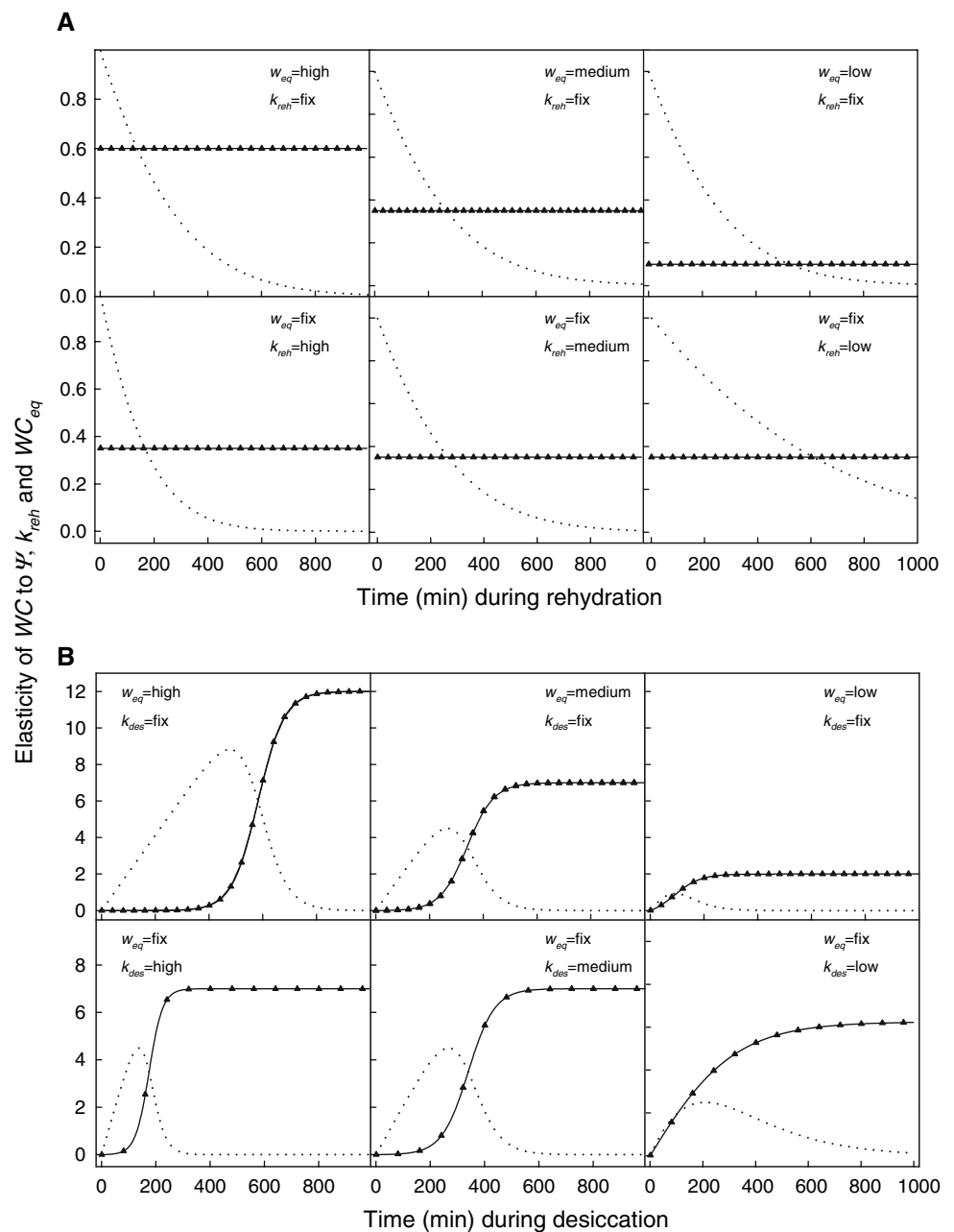

still very precise for *A. sarmentosa* (Table 4). For the other two species, the models overestimated the shorter events and underestimated the longer ones. In general, the biophysical model tended to simulate the hydration period lengths with a higher accuracy than the physical model during humid air, as judged from the slope values of the simulated to observed regression equation (Table 4).

Timing of hydrated periods

To analyze how accurately the models could predict the timing of the hydration events, data were again separated between periods induced by rain or by humid air, as above,

and presented as time-overlaps between the observed and simulated hydration periods (Fig. 7). In general, the timing was better for the long hydration periods induced by rain (Fig. 7a–d) than for the short periods induced by humid air (Fig. 7e–h), with the highest accuracy for *A. sarmentosa* and the lowest for the embedded *C. rangiferina* samples. The timing of the rain events was better predicted by the physical model than by the biophysical model (Fig. 7a–d), while the biophysical model was a better predictor of the humid air events (Fig. 7e–h).

The accumulated hydration period ranged from approximately 1100 hours for the two epiphytic lichens to approximately 1900 hours for the embedded *C. rangiferina*
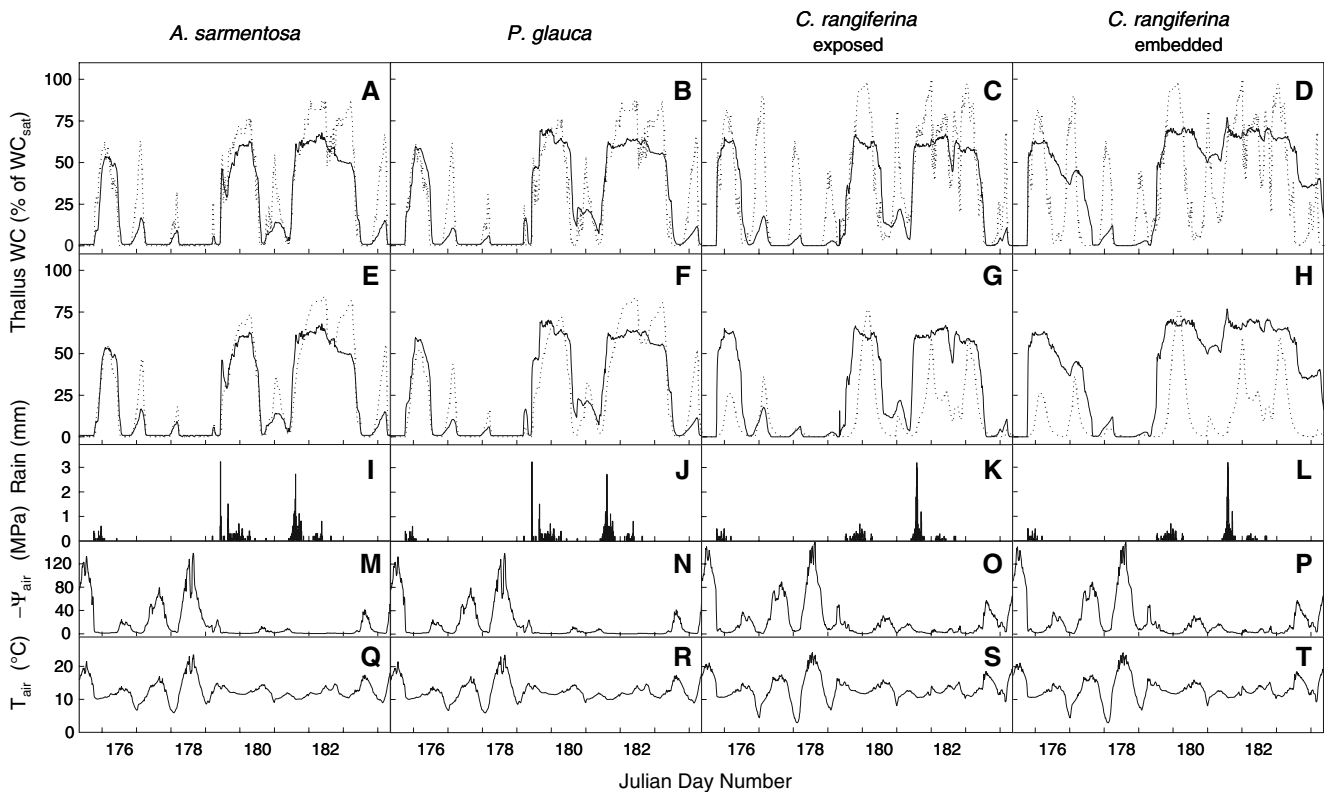
Fig. 5 Measured (*solid line*) and simulated (*dotted line*) thallus WC (**a–h**) resulting from the physical model (**a–d**) and the biophysical model (**e–h**), and precipitation (**I–l**), ψ_{air} (**m–p**) and T_{air} (**q–t**), between June 23 and July 2, 2004 (Julian Day number 175–184) for *A. sarmentosa*, *P. glauca* and *C. rangiferina* (exposed and embedded thalli separately). Observed thallus WC data are the average of exposed and shaded thalli at the respective measurement sites (see Table 1). The simulations were made for an independent data set at Kulbäcksliden (*A. sarmentosa* and *P. glauca*) and Åheden (*C. rangiferina*) (Table 1). See Table 2 for definitions of abbreviations and constants

(Table 4), while the duration of the experimental period was approximately 2500 h. Both models simulated a total hydration time that was very close to the observed one for the epiphytic lichens, with approximately 90% of the simulated wet time occurring when *A. sarmentosa* or *P. glauca* was observed to be wet (Table 4). The accuracy of the models to simulate the total wet time was lower for *C. rangiferina* and particularly low for the embedded samples of this lichen (Table 4).

Discussion

The results of this study reveal that water relations of lichens can be simulated using mathematical models and measurements of the water potential of the air in combination with a few species-specific characteristics (Eqs. 3–5, Fig. 3, Table 3). These models were able to continuously simulate the constantly varying water status over a 3.5-month-long period (Fig. 5, Table 4), with an accurate timing (Fig. 7, Table 4), and in a contrasting habitat compared to the parameterization site (Table 1, Fig. 5).

This result emphasizes that the water status of lichens can be predicted over long periods and under contrasting weather conditions without explicit precipitation data. However, our developed models were more precise for the epiphytic lichens *A. sarmentosa* and *P. glauca* than for the terricolous *C. rangiferina* (Figs. 5, 6, 7, Tables 3, 4), as hypothesized, suggesting that the models need to be further developed for terriculous lichens.

There are numerous studies on lichen water relations (Blum 1973; Rundel 1982; Lange et al. 1986, 1993, 2006; Green et al. 1991, 1994; Zotz et al. 1998; Lalley and Viles 2006), and attempts to predict lichen field water relations have previously been carried out. However, the aim of these other studies was not to explicitly predict the length and occurrence of wet active periods of lichens in field conditions. On the other hand, previous models were also able to predict the uptake of various water sources (Paterson et al. 1983; Pech 1989) and/or the mechanistic loss of water (Kershaw and Harris 1971; Lloyd 2001) and/or prediction by meteorological variables (Kershaw and Harris 1971; Paterson et al. 1983; Pech 1989; Lloyd 2001). Therefore, the major advantage of the models presented
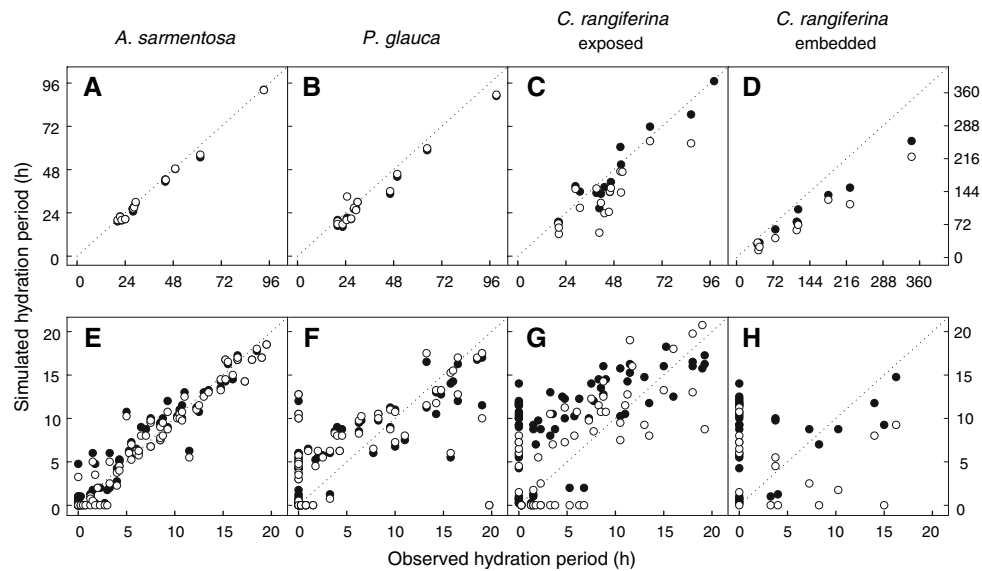
Fig. 6 Length of all simulated hydration periods (WC >5%), separated into rain events (>20 h) (**a–d**) and humid air events (<20 h) (**e–h**), using the physical model (*closed symbols*) and the biophysical model (*open symbols*), as a function of measured lengths for *A. sarmentosa* (**a**, **e**), *P. glauca* (**b**, **f**) and exposed (**c**, **g**) and embedded *C. rangiferina* (**d**, **h**). The *dotted line* in each graph represents a theoretical optimal 1:1 fit between observed and simulated data. Measurements and simulations were made using data from different sites as detailed in Table 1 and for the whole experimental period. Parameters of the linear regressions fitted to each data series are presented in Table 4

here is the combination of few relatively easily obtained variables that catch all sources of water while still being mechanistic. This has resulted in dynamic and continuous simulations. Although the physical model worked well, the incorporation of species-specific characters in the biophysical model facilitates predictions concerning, for example, differences in distribution patterns between species.

Model behavior in relation to water source

Lichens are only active and can hence only grow when they are sufficiently hydrated (see Palmqvist 2000). Models of their productivity must therefore be able to predict both the length and timing of these periods. The model must also cover the different water sources—rain, humid air, fog or dew—since at least the green algal lichens can be activated by all of these various forms (Kershaw and Rouse 1971a; Lange et al. 1988). However, due to the general patterns of faster activation of metabolism by rain compared to humid air and the potentially higher metabolic activity reached during these events (see Palmqvist 2000 and references therein), for many species, one might assume that it is of particular importance that the rain-induced hydration periods are well predicted. This being said, we know that a number of species display distribution patterns, for example, confinement to habitats close to turbulent water (Lidén and Hilmo 2005), which indicates that other sources of

humidity than precipitation may be very important for their metabolic output (Kappen et al. 1980; Lange et al. 1986, 1988, 2001; Lidén and Hilmo 2005).

The models presented here simulated the rain-induced hydration periods accurately for all three species (Figs. 6a–d, 7a–d, Table 4), although they somewhat underestimated the observed values. The physical model had a higher accuracy during rain than the biophysical model. This is not surprising since hydration by rain occurs within minutes (Blum 1973; Rundel 1988), and the assumption of an instantaneous WC equilibrium, such as in the physical model, is more appropriate when modeling water uptake during rain (compare Fig. 5c, g, day 179). In contrast, the water uptake by humid air requires a longer equilibration process and was therefore more accurately described by the biophysical model (compare Fig. 5c, g, evening 177). However, the humid air-induced periods were generally overestimated (Table 4), particularly the very shortest ones (Fig. 6e–h). This may be explained by the procedure used to parameterize the equilibrium WC level (Eq. 3) whereby rehydration by high RH was assumed to potentially result in fully water-saturated thalli, which according to the literature (Smith 1962; Lange et al. 1986,) is in itself an overestimation.

A partitioning between the rain and the humid air events in the parameterization would therefore improve the modeling. However, this step would include the added complexity of keeping track of different water sources during data collection, parameterization and simulations.

Table 4 Parameters of the linear regressions presented in Fig. 6 and additional observations on the total simulated and measured wet time and timing

Model	A. sarmentosa	P. glauca	C. rangiferina	
			Exposed	Embedded
Rain events (>20 h)				
Biophysical				
Slope (b)	0.981 ± 0.026	0.915 ± 0.022	0.77 ± 0.130	0.636 ± 0.039
Intercept (y_0)	-1.22 ± 1.07	-0.19 ± 1.51	0.46 ± 5.99	-5.70 ± 6.20
Adjusted r^2	0.99	0.99	0.68	0.97
Physical				
Slope (b)	0.982 ± 0.021	0.917 ± 0.015	0.971 ± 0.089	0.734 ± 0.032
Intercept (y_0)	-0.92 ± 0.88	-1.68 ± 1.03	-0.58 ± 4.59	-1.36 ± 5.09
Adjusted r^2	0.99	>0.99	0.89	0.98
Humid air events (<20 h)				
Biophysical				
Slope (b)	0.954 ± 0.028	0.604 ± 0.073	0.817 ± 0.104	-0.105 ± 0.172
Intercept (y_0)	0.16 ± 0.25	3.06 ± 0.63	2.28 ± 0.93	5.10 ± 1.26
Adjusted r^2	0.94	0.52	0.56	0.000
Physical				
Slope (b)	0.919 ± 0.029	0.529 ± 0.073	0.618 ± 0.081	0.221 ± 0.159
Intercept (y_0)	0.84 ± 0.26	3.75 ± 0.62	6.07 ± 0.63	7.27 ± 0.83
Adjusted r^2	0.92	0.45	0.44	0.026
Additional observations				
Measured tot wet time (h)	1062	1057	1381	1874
Simulated tot wet time (h [%])				
Physical model	1,068 (100.5)	1049 (99.2)	1643 (119.0)	1643 (87.7)
Biophysical model	1026 (96.5)	1047 (99.1)	1215 (88.0)	1215 (64.8)
Time overlap of simulated vs measured wet periods (%)				
Physical model	92.4	83.1	86.3	70.0
Biophysical model	92.6	85.5	73.2	56.4

Data were separated between hydration events shorter or longer than 20 h in order to separately analyze hydration periods resulting from humid air or rain, respectively. Data were fitted to a linear regression equation of the form $y = y_0 + bx$. The intercept (y_0) and slope of the line (b) with the confidence interval $\pm$ 1 SE and adjusted r^2 for the species-specific simulated versus observed data are presented for both the biophysical and the physical model for A. sarmentosa, P. glauca, and separated exposed and embedded C. rangiferina. All slopes were significant at $P < 0.001$, with the exception of embedded C. rangiferina for periods <20 h (physical $P = 0.175$, biophysical $P = 0.550$). Moreover, additional observations for measured and simulated total wet time and the timing of these periods are expressed as time overlap (see Fig. 7) using the physical and the biophysical models, respectively, for the whole experimental period (3.5 months = 2568 h) for A. sarmentosa, P. glauca and separated exposed and embedded C. rangiferina

Values in parenthesis represent the percentage of the simulated wet time in relation to the measured. The measured wet time represents the mean of the "validation thalli" (see Table 1)

Model success in relation to species

The models simulated the water relations of A. sarmentosa and P. glauca with a higher precision than they simulated those of C. rangiferina (Fig. 5, 6, 7; Table 4). This may be explained by the structure of these models. For successful WC simulations, these models rely on a high coupling between lichen and atmospheric water potentials. The epiphytic lichens were more exposed to the atmospheric conditions since they lack significant boundary layers. In contrast, C. rangiferina was harder to predict due to the boundary layer formed by its mat-forming growth form. Lichens with substantial boundary layers will likely prolong their hydration periods (Kershaw and Field 1975; Larson and Kershaw 1976; Gates 1980; Zotz et al. 2000), especially in sheltered positions (Nash et al. 1977; Kappen et al 1980; Rundel 1982). The lower accuracy for these lichens and such situations is expected by the equilibrium model of Monteith (1965), which states that for water-saturated conditions, as may be the case within boundary layers, net radiation rather than atmospheric water potential drives water loss. The exposed C. rangiferina was,
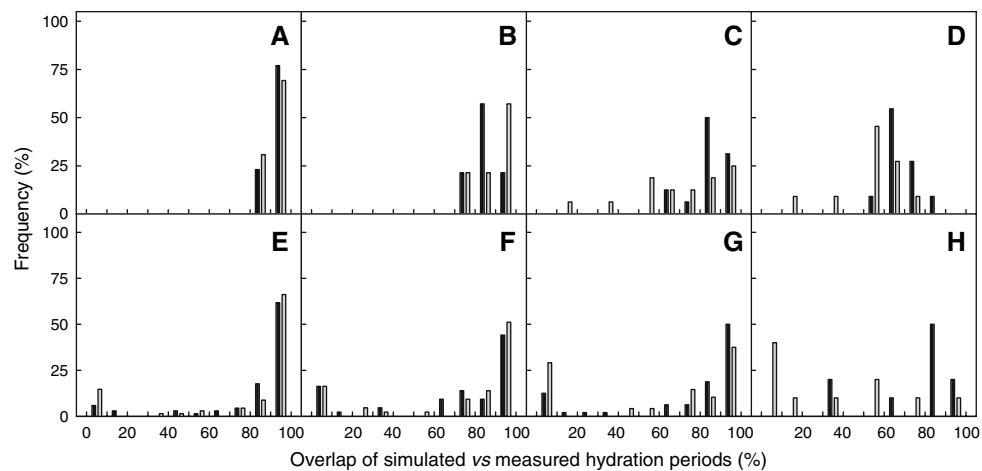
Fig. 7 Timing of simulated versus measured hydration periods (WC >5%), separated into rain events (>20 h) (**a–d**) and humid air events (<20 h) (**e–h**), using the physical model (*black bars*) and the biophysical model (*grey bars*), as a function of measured lengths for *A. sarmentosa* (**a**, **e**), *P. glauca* (**b**, **f**) and exposed (**c**, **g**) and embedded *C. rangiferina* (**d**, **h**). Timing is presented as time-overlaps of the two data sets and in the step-wise intervals 0–10, 10–20, 20–30, 30–40, 40–50, 50–60, 60–70, 70–80, 80–90 and 90–100% overlap. When simulated hydration periods overlapped the measured ones completely, the overlap was defined as 100%. Measurements and simulations were made using data from different sites, as detailed in Table 1, and for the whole experimental period

however, more accurately predicted than the embedded *C. rangiferina*, probably due to a reduced boundary layer in the former by winter grazing reindeer. This grazing would enhance the coupling between the lichen and the atmospheric water conditions (Rice et al. 2001), thus facilitating more precise WC simulations by the models presented here. To improve WC simulations of embedded lichens, the model should include an additional term for boundary layer conditions where net radiation drives evaporative loss.

Elasticity analysis

Based on the elasticity analysis of the biophysical model (Fig. 4), lichen WC depends on the species-specific rehydration and desiccation processes only until equilibrium with the atmosphere is reached. Once equilibrium is reached, the WC level is dependent on the ψ_{air} and w_{eq}. This implies that species with fast equilibration processes, such as *A. sarmentosa* and *P. glauca*, are mostly controlled by the environmental conditions and the specific water content at equilibrium. This outcome confirms the logical interpretation of Eq. 3 and, consequently, since the two epiphytic species had rapid water uptake and loss rates (Table 3), typical for fruticose and thin-lobed thalli (Larson and Kershaw 1976; Larson 1981), the difference was minimal between the two models. This emphasizes that those species can be sufficiently modeled by the physical model without the more mechanistic equilibration processes incorporated in the biophysical model.

In line with the above discussion, the biophysical model should theoretically be better than the physical model for *C. rangiferina*, due to its slower equilibration processes

(Table 3). However, the physical model, which generally predicted the rain events better than the biophysical model, did so also for *C. rangiferina* (Figs. 5, 6, 7, Table 4). This implies that conclusions regarding parameter sensitivity among species can not be based solely on the elasticity analysis (Fig. 4) but that they must also consider the ability of the models to track different water sources (Figs. 6, 7; Table 4).

Model assumptions

The biophysical model presented here is related to the mechanistic hydration model and theories presented by Rundel (1982). However, in contrast to that model, we assumed that both uptake and loss of water are related to ψ_{air} and that thallus WC was mainly affected by this factor. This is an over-simplification because thallus hydration status can also be affected by the osmotic potential of the thallus (Nash et al. 1990; Hajek et al. 2006) or by thallus color in combination with solar radiation, both of which influence thallus temperature (Kershaw 1975) and consequently thallus water potential more than expected by atmospheric conditions alone. Since we can not measure or estimate the true water potential of the lichen thallus in situ, the lack of agreement between atmospheric and thallus water potential can not be considered in these models. This may be more important for dark, foliose lichens in exposed habitats with small boundary layers, since boundary layers may counteract the increased rate of water loss. On the other hand, the equation of the ψ_{air}–WC_{eq} relation (Eq. 3) also contained a constant (w_{eq}) sensitive to the specific water content at equilibrium (Fig. 2, Table 3),

where the osmotic potential and structure of the thallus may well be important components. Since variation in w_{eq} also had a significant impact in the elasticity analysis, affecting the equilibration time during rehydration and desiccation (Fig. 4), it would be interesting to explore this parameter better, particularly for species in sheltered habitats.

The aim of this study was to construct a model to predict the wet and active periods. These periods can then be combined with the prevailing irradiance for correlation with lichen growth (Palmqvist and Sundberg 2000; Dahlman and Palmqvist 2003). However, to assess the instantaneous metabolic rates, a more precise lichen water content is also required (Lange 1980; Green et al. 1994; Lange et al. 1986, 1993; Lange and Green 1996). Our developed models have not been adjusted to fit exact WC levels although the simulations apparently also catch the dynamics near maximum water content. For that purpose, the models would likely be improved by separating the humid air and rain events in the parameterization, as already discussed. However, this step would bring a complexity to the model that may not always be required for predicting the active and potential growth periods of lichens.

Despite the rather simple modeling approach, the high precision already obtained by our two models opens up new possibilities for using modeling as a tool to predict water relations of lichens in various habitats. This has important ecological applications for understanding the complex interactions between macro- and microclimatic sources of humidity and lichen responses. We also suggest that the models presented here may be used for understanding the underlying factors that limit lichen species distributions or responses to altered environmental conditions.

References

Blum OB (1973) Water relations. In: Ahmadjian VV, Hale ME (eds) The lichens. Academic Press, New York, pp 381–400

Coxson D (1991) Impedance measurement of thallus moisture content in lichens. Lichenologist 23:77–84

Dahlman L, Palmqvist K (2003) Growth in two foliose tripartite lichens Nephroma arcticum and Peltigera aphthosa—empirical modelling of external versus internal factors. Funct Ecol 17:821–831

Epstein HE, Calef MP, Walker MD, Chapin FS, Starfield AM (2004) Detecting changes in arctic tundra plant communities in response to warming over decadal time scales. Glob Change Biol 10:1325–1334

Esseen PA, Renhorn KE, Petersson RB (1996) Epiphytic lichen biomass in managed and old-growth boreal forests: effect of branch quality. Ecol Appl 6:228–238

Fos S, Deltoro VI, Calatayud A, Barreno E (1999) Changes in water economy in relation to anatomical and morphological characteristics during thallus development in Parmelia acetabulum. Lichenologist 31:375–387

Gaio-Oliveira G, Dahlman L, Máguas C, Palmqvist K (2003) Growth in relation to microclimatic conditions and physiological characteristics of four Lobaria pulmonaria populations in two contrasting habitats. Ecography 27:13–28

Gaio-Oliveira G, Moen J, Danell Ö, Palmqvist K (2006) Effect of simulated reindeer grazing on the re-growth capacity of mat-forming lichens. Basic Appl Ecol 7:109–121

Gates DM (1980) Biophysical ecology. Springer, Berlin

Gauslaa Y, Solhaug KA (1998) The significance of thallus size for the water economy of the cyanobacterial old-forest lichen Degelia plumbea. Oecologia 116:76–84

Green TGA, Kilian E, Lange OL (1991) Pseudocyphellaria dissimilis: a desiccation-sensitive, highly shade-adapted lichen from New Zealand. Oecologia 85:498–503

Green TGA, Lange OL, Cowan IR (1994) Ecophysiology of lichen photosynthesis: the role of water status and thallus diffusion resistances. Cryptogam Bot 4:166–178

Hajek J, Bartak M, Dubova J (2006) Inhibition of photosynthetic processes in foliose lichens induced by temperature and osmotic stress. Biol Plant 50:624–634

Heatwole H (1966) Moisture exchange between the atmosphere and some lichens of the genus Cladonia. Mycologia 58:148–156

Kappen L, Lange OL, Schultze ED, Buschbom U, Evenari M (1980) Ecophysiological investigations on lichens of the Negev desert VII. The influence of the habitat exposure on dew imbibition and photosynthetic productivity. Flora 169:216–229

Kershaw KA (1975) Studies on lichen-dominated systems. XII. The ecological significance of thallus color. Can J Bot 53:660–667

Kershaw KA, Field GF (1975) Studies on lichen-dominated systems. XV. The temperature and humidity profile in a Cladina alpestris mat. Can J Bot 53:2614–2620

Kershaw KA, Harris GP (1971) Simulation studies and ecology: a simple defined system model. Stat Ecol 3:1–21

Kershaw KA, Rouse WR (1971a) Studies on lichen-dominated systems. I. The water relations of Cladonia alpestris in spruce-lichen woodland in northern Ontario. Can J Bot 49:1389–1399

Kershaw KA, Rouse WR (1971b) Studies on lichen-dominated systems. II. The growth pattern of Cladonia alpestris and Cladonia rangiferina. Can J Bot 49:1401–1410

Kumpula J (2001) Winter grazing of reindeer in woodland lichen pasture. Effect of lichen availability on the condition of reindeer. Small Rumin Res 39:121–130

Lalley JS, Viles HA (2006) Do vehicle track disturbances affect the productivity of soil-growing lichens in a fog desert? Funct Ecol 20:548–556

Lange OL (1980) Moisture content and CO_2 exchange in lichens. I. Influence of temperature on moisture dependent net photosynthesis and dark respiration in Ramalina maciformis. Oecologia 45:82–87

Lange OL, Green TGA (1996) High thallus water content severely limits photosynthetic carbon gain of central European epilithic lichens under natural conditions. Oecologia 108:13–20

Lange OL, Kilian E, Ziegler H (1986) Water vapor uptake and photosynthesis of lichens: performance differences in species with green and blue-green algae as phycobionts. Oecologia 71:104–110

Lange OL, Green TGA, Ziegler H (1988) Water status related photosynthesis and carbon isotope discrimination in species of the lichen genus *Pseudocyphellaria* with green or blue-green photobionts and in photosymbiodemes. Oecologia 75:494–501

Lange OL, Büdel B, Heber U, Meyer A, Zellner H, Green TGA (1993) Temperate rainforest lichens in New Zealand: high thallus water content can severely limit photosynthetic CO_2 exchange. Oecologia 95:303–313

Lange OL, Green TGA, Heber U (2001) Hydration-dependent photosynthetic production of lichens: what do laboratory studies tell us about field performance? J Exp Bot 52:2033–2042

Lange OL, Green TGA, Melzer B, Meyer A, Zellner H (2006) Water relations and CO_2 exchange of the terrestrial lichen *Teloschistes capensis* in the Namib fog desert: measurements during two seasons in the field and under controlled conditions. Flora 201:268–280

Larson DW (1981) Differential wetting in some lichens and mosses: the role of morphology. Bryologist 84:1–15

Larson DW, Kershaw KA (1976) Studies on lichen-dominated systems. XVIII. Morphological control of evaporation in lichens. Can J Bot 54:2061–2073

Lidén M, Hilmo O (2005) Population characteristics of the suboceanic lichen *Platismatia norvegica* in core and fringe habitats: relations to macroclimate, substrate, and proximity to streams. Bryologist 108:506–517

Lloyd CR (2001) The measurement and modelling of the carbon dioxide exchange at a high Arctic site in Svalbard. Glob Change Biol 7:405–426

Maguás C, Valladares F, Brugnoli E (1997) Effects of thallus size on morphology and physiology of foliose lichens: new findings with a new approach. Symbiosis 23:149–164

Monteith JL (1965) Evaporation and environment. Symp Soc Exp Biol 19:205–234

Mutch RW, Gastineau OW (1970) Timelag and equilibrium moisture content of reindeer lichen. USDA For Serv Res Pap INT-76. Forest and Range Experimental Station, Odgen, UT

Nash III TH, Reiner A, Demmig-Adams B, Kilian E, Kaiser WM, Lange OL (1990) The effect of atmospheric desiccation and osmotic water stress on photosynthesis and dark respiration of lichens. New Phytol 116:269–276

Nash III TH, White SL, Marsh JE (1977) Lichen and moss distribution and biomass in hot desert ecosystems. Bryologist 80:470–479

Nobel PS (1999) Physicochemical and environmental plant physiology, 2nd edn. Academic Press, San Diego

Palmqvist K (2000) Carbon economy in lichens. New Phytol 148:11–36

Palmqvist K, Sundberg B (2000) Light use efficiency of dry matter gain in five macro-lichens: relative impact of microclimate and species-specific traits. Plant Cell Environ 23:1–14

Paterson DR, Paterson EW, Kenworthy JB (1983) Physiological studies on temperate lichen species I. A mathematical model to predict assimilation in the field, based on laboratory responses. New Phytol 94:605–618

Pech GY (1989) A model to predict the moisture content of reindeer lichen. For Sci 35:1014–1028

Renhorn K-E, Esseen P-A, Palmqvist K, Sundberg B (1997) Growth and vitality of epiphytic lichens. I. Responses to microclimate along a forest edge-interior gradient. Oecologia 109:1–9

Rice SK, Collins D, Anderson AM (2001) Functional significance of variation in bryophyte canopy structure. Am J Bot 88:1568–1576

Rundel PW (1982) The role of morphology in the water relations of desert lichens. J Hattori Bot Lab 53:315–320

Rundel PW (1988) Water relations. In: Galun M (ed) CRC handbook of lichenology, vol 2. CRC Press, Boca Raton, pp 17–36

Saunders DA, Hobbs RJ, Margules CR (1991) Biological consequences of ecosystem fragmentation: a review. Conserv Biol 5:18–32

Schroeter B, Scheidegger C (1995) water relations in lichens at subzero temperatures: structural changes and carbon dioxide exchange in the lichen *Umbilicaria Aprina* from continental Antarctica. New Phytol 131:273–285

Smith DC (1962) The biology of lichen thalli. Biol Rev 37:537–570

Sundberg B, Näsholm T, Palmqvist K (2001) The effect of nitrogen on growth and key thallus components in the two tripartite lichens, *Nephroma arcticum* and *Peltigera aphthosa*. Plant Cell Environ 24:517–527

Söchting U (1995) Lichens as monitors of nitrogen deposition. Crypt Bot 5:264–269

Valladares F (1994) Texture and hygroscopic features of the upper surface of the thallus in the lichen family *Umbilicariaceae*. Ann Bot 73:493–500

Valladares F, Wierzchos J, Ascaso C (1993) Porosimetric study of the lichen family *Umbilicariaceae*: anatomical interpretation and implications for water storage capacity of the thallus. Am J Bot 80:263–272

Zotz G, Büdel B, Meyer A, Zellner H, Lange OL (1998) In situ studies of water relations and CO_2 exchange of the tropical macrolichen, *Sticta tomentosa*. New Phytol 139:525–535

Zotz G, Schweikert A, Jetz W, Westerman H (2000) Water relations and carbon gain are closely related to cushion size in the moss *Grimmia pulvinata*. New Phytol 148:59–67